

Composite thin circular plates undergo a dramatic change in their dynamic behavior upon incorporation of cuts

Dr.B.H.Manjunath, Chandrakumar.C, Murthy.S.L

Prof. & HOD, Asst. Prof, Asst. Prof

bhmanj@gmail.com, chakrapdit@gmail.com, murthypdit@gmail.com

Department of Mechanical, Proudhadivaraya Institute of Technology, Abheraj Baldota Rd,

Indiranagar, Hosapete, Karnataka-583225

ABSTRACT

Its effect on the fundamental frequency and harmonic response is investigated in relation to the cut-out form. delicate composite sheets with round forms and evenly formed perimeters. This formerly used module is based on ANSYS Workbench 18.2's Finite Element Method. With an equilateral triangle in the centre, the nine separate spherical plates have square, pentagon, hexagon, heptagon, and octagon shapes. Normal nonagon, decagon, and circle patterns were built to study the evolution of the building's vibratory response as the opening geometry approaches a circle. Plus, a strong circular plate was made so that measurements could be taken and compared. We need more thorough research on the consequences of the slit shape since the structures are designed using cross-ply and angle-ply composites. Without charging you a dime, we have completed the vibration research. that each structure's basic tone frequency may be determined. Methods for completing the harmonic response analysis are detailed here. combine a predetermined damping ratio with the Mode Superposition Technique. It is possible to make sense of these study findings by thinking about stress, displacement reaction, and frequency-dependent phase changes. According to the research, the cut-forms of the spherical framework significantly impact the fundamental frequency and harmonic response, independent of the fibre orientation.

Keywords:

Frequency of harmonic resonance; Geometry of cutouts; Modeling using discrete elements.

INTRODUCTION

Numerous technical uses have made use of holes in circular plates. Many studies on the vibrational properties of these structures have been motivated by their susceptibility to stresses that may lead to their collapse. resonance, a phenomena that leads to the collapse of buildings. Additionally, these structures may be damaged by the incredible stress and displacement caused by the high vibration caused by these loads. (Sivandi-Pour et al., 2020; elebi et al., 2018; albas Sam., 2021) and Gonenli & Das, 2021) are only a few of the studies that have evaluated structural vibration using methods like harmonic response analysis. Kumar and Sarangi (2019), Liu et al. (2021), and Son et al. (2021) are a few studies that have been touched on briefly yet are crucial to this topic. The following must be considered. The vibration response characteristics that show the movement of a damaged compressor blade were examined by Zeng et al. (2019) using Finite Element Analysis. Kral investigated the harmonic and resonant behavior of laminated composites (2014). beams that are placed through different confinement sequences and boundary conditions. How a composite beam reacts while something is in motion. Gawryluk et al. (2019) found that it spins at a steady pace. The harmonic response of cross-ply and angle-ply composites of varying materials and thicknesses was investigated by Abed and Majeed (2020) in relation to boundary conditions. Carbon Fiber Laminate Reinforced Concrete Railway Sleepers were studied by even and Aktaş in terms of their modal and harmonic responses (2021). focused their study on the dynamic response of fluid-transporting composite pipes,

Oka and Khalif (2020) zeroed focused on a discontinuity in the inner wall surface. Harmonic analysis of coupled plate structures was carried out by Zhang et al. (2018) using the dynamic stiffness approach. Yuling et al. (2020) studied the dynamic response of a three-beam system supported by mass springs when subjected to a moving load.

CIRCULAR STRUCTURES AND THE FINITE ELEMENT APPROACH

In order to assess the fundamental natural frequency and the harmonic response of the composite thin circular plates shown in Figure 1, the Finite Element Analysis has been used. A structure's equation of motion looks like this:

$$M\ddot{\delta} + C\dot{\delta} + K\delta = F$$

where the mass, damping, and stiffness matrices are denoted by M, C, and K respectively. The vector F is the external force, while the vector is the generalized displacement coordinates. Various textbooks discuss how to evaluate certain matrices and vectors (Petty, 2010). When calculating a structure's basic natural frequency, it is important to assume that no external force is acting on it and that the damping is also zero. The resulting equation of motion is.

$$M\ddot{\delta} + K\delta = 0$$

Reducing Equation (2) into an eigenvalue problem gives

$$(K - \omega_l^2 M)\psi_l = 0$$

the itch natural frequency of the examined structure, and the itch mode shape, the external force and the resulting reaction must be harmonic for the structure to exhibit what is known as a "harmonic response." Taking the complicated external force into consideration as

$$F = F_{max}e^{j\mu}e^{j\Omega t}$$

and the displacement response as

$$r = r_{max}e^{j\gamma}e^{j\Omega t}$$

where Ω is the excitation frequency, γ and μ are the phase shifts of the force and response, respectively. Substituting Equation (5) into Equation (1) and reducing it to eigenvalue problem give

$$(K + j\Omega C - \Omega^2 M)\psi_l = F$$

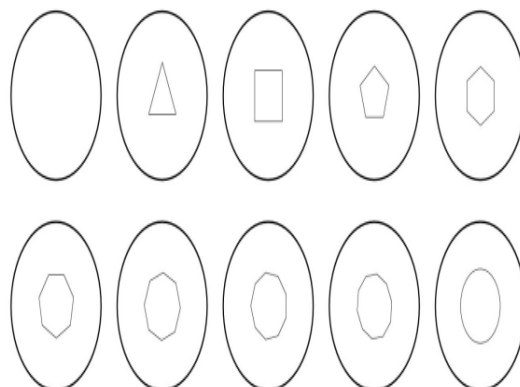
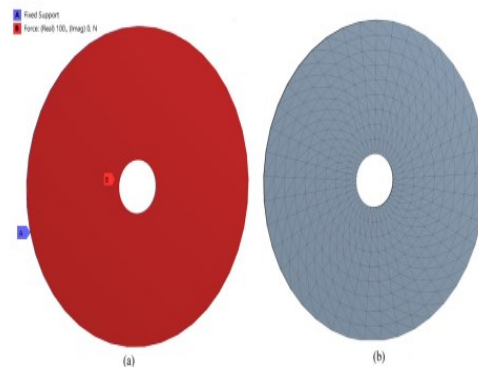


Figure 1. Thin composite circular plates.

The response of the structure may be determined by solving Equation (5) with the frequencies determined by the findings of Equation (3) (Petty, 2010). Free vibration and harmonic response analyses have been considered using the SHELL181 module of ANSYS Workbench. A triangular element with six degrees of freedom has been the object of our investigation for meshing purposes. Due of the small maximum allowable mesh size of 7 mm, the adaptive mesh method was used. The perimeters of all structures were reinforced. In order to conduct the harmonic response investigation, the top surfaces of each structure were tested with a sinusoidal force that could reach a maximum magnitude of 100 N. To see the boundary condition, harmonic force, and mesh structure employed in



this situation, see Figure 2.

Figure 2. (a) The boundary condition and applied harmonic load; (b) meshed structure.

Because it is both faster and more accurate than the Full Method, the Mode Superposition Method was used to solve the harmonic response analysis. The Mode Superposition method requires the eigenvectors, sometimes called mode forms, which may be obtained by a free vibration analysis. In order to assess the impact of the cut-out shape on the fundamental frequency and fulfill the requirements given above, free vibration analysis was performed on all structures with the same boundary conditions. By doubling the fundamental frequency by 1.5, the frequency range was determined to ensure that the response could be perceived. Results may be more accurately predicted when the damping effect, as shown by the material damping coefficient of =0.02 (Kraal, 2014), is included. Graphs representing crucial frequencies, displacements, phases, and stresses have all been examined.

STATISTICAL CONCLUSIONS

The examined circular structure's geometric features are listed in Table 1. Epoxy carbon composite with a single direction of carbon Fiber has been proposed as the composite material. The following are some characteristics of the material: Where $E_x= 121$ GPa, $E_y= 8.6$ GPa, $G_x= 4.7$ GPa, $G_{yz}= 3.1$ GPa, $\nu_{xy}= \nu_{xz}= 0.27$, $\nu_{yz}= 0.4$, where E_x , E_y , and E_z are the modulus of elasticity with respect to the x-, y-, and z-axes, G_x , G_{xz} , and G_{yz} are the shear modulus with regard to the.

Table 1. Geometrical properties of considered structures

Property	Symbol	Value
Circular Plate Diameter	d	300 mm
Circular Plate Thickness	t	3 mm
Cut-Out Area	A_c	1963.5 mm ²

It was feasible to examine the effect of the cutout on the design by smoothing out its edges. The roughness has been drastically reduced, going from an equilateral triangle to a circular shape, by expanding the number of edges from three to an infinite number. The constant cut-out area was calculated using a circular cut-out of 50 mm diameter in mind. The design of all following apertures was inspired by this permanent cut-out part. The cut-outs have different lengths of edges and different areas (1963.5 mm²). Sun et al. (2021) checked their results to these to make sure they are correct. For this purpose, five-layer composite circular plates with 100 x 100 mm, 200 x 200 mm, and 300 x 300 mm square cut-outs, 1000 mm in diameter and 10 mm thick, were tested. The layers used were 00, 300, 450, 600, and 900. Sun et al. (2021) provides a comprehensive account of the material properties in their corresponding study. Using the nondimensional fundamental frequency, $\omega_n = 512 \cdot d \cdot \sqrt{E_1 / (1 - \nu_{12} \nu_{21})}$, a comparative study was conducted, and the results are shown in Table 2. (Sun et al., 2021) The formula $(1 / \omega_n) \cdot \sqrt{E_1 / (1 - \nu_{12} \nu_{21})}$ takes into account the natural frequency, diameter (d), modulus of elasticity (E1) of the composite material with respect to the x-axis, and Poisson's ratios (ν_{12} and ν_{21}). **Table 2. Nondimensional comparative analysis results (Cs: cut-out size).**

Frequency Mode	Cs=100x100 mm		Cs=200x200 mm		Cs=300x300 mm	
	Present Study (ANSYS)	Sun et al. (2021)	Present Study (ANSYS)	Sun et al. (2021)	Present Study (ANSYS)	Sun et al. (2021)
1	13.8769	14.0171	14.6178	14.9673	16.8574	17.2956
2	27.7943	27.7297	26.3399	26.9835	25.5896	26.3601
3	28.4032	28.3875	26.8451	27.5683	25.9336	26.8029
4	44.0324	44.3372	41.6928	42.6750	40.7880	41.8831
5	45.4892	45.1408	42.7731	43.4541	41.3441	42.4390

Table 2 shows that the considered method's free vibration findings are quite consistent with those of Sun et al (2021). The cut-out forms of thin cross ply and angle-ply circular plates are shown in Table 3, and their corresponding fundamental frequencies are listed in Table 4.

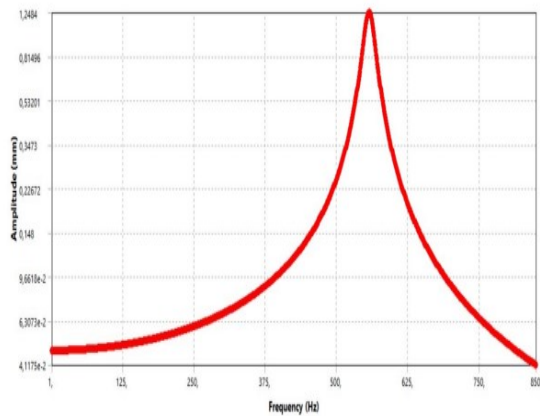
Table 3. Nondimensional fundamental frequencies of cross-ply circular plates.

Frequency (ω_n)	No Cut-Out	Equilateral Triangular Cut-Out	Square Cut-Out	Regular Pentagon Cut-Out	Regular Hexagon Cut-Out
1	106.6451	136.1910	150.6220	141.9210	150.1756
Frequency (ω_n)	Regular Heptagon Cut-Out	Regular Octagon Cut-Out	Regular Nonagon Cut-Out	Regular Decagon Cut-Out	Circular Cut-Out
1	155.9056	146.6802	144.7556	161.6618	155.3028

Table 4. Nondimensional fundamental frequencies of angle-ply circular.

Frequency (f_{nat})	No Cut-Out	Equilateral Triangular Cut-Out	Square Cut-Out	Regular Pentagon Cut-Out	Regular Hexagon Cut-Out
1	106.3524	135.9156	150.6219	141.7298	150.1234
Frequency (f_{nat})	Regular Heptagon Cut-Out	Regular Octagon Cut-Out	Regular Nonagon Cut-Out	Regular Decagon Cut-Out	Circular Cut-Out
1	155.6622	146.5787	144.7093	161.4241	155.2158

Tables 4 and 5 indicate that compared to the identical plates without cutouts, the fundamental natural frequencies of the circular plates with cutouts are higher. Adding additional regular shapes (such as pentagons, octagons, and nonagons) to the structure causes the frequency value to decline, even if it seems to be going up. By comparing the two cut-outs with varying numbers of edges, it is shown that the fundamental frequency of the circular construction with a circular cutout is much higher than that of the equilateral triangle cutout. The results show that compared to the structure with the cross-ply Fiber sequence, the one with the angle-ply Fiber orientation has slightly lower fundamental frequencies (approximately 1Hz). Table 5 displays the values of the maximum stress and displacement, together with the phase shift, while Table 6 displays the results of the harmonic response analysis. In Figure 3, we can see the frequency response and frequency phase diagram of the circular cross-ply plate with the regular decagon cut-out centrally shown. It should be noted that all other structures have the same frequency response and phase. Only changes in frequency, responsiveness, and phase may be identified. The most intense responses were seen at the basic frequency of every structure, as shown in Figure 3(a). The phase shift is observed at the fundamental frequency for all spherical structures.



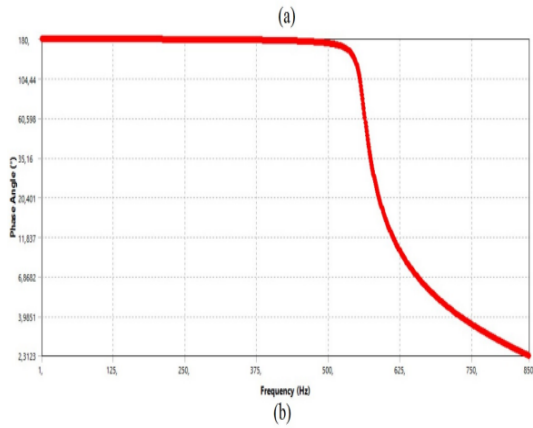


Figure 3. (a) The frequency-displacement response and (b) frequency-phase diagram of cross-ply circular plate having central regular decagon cut-out.

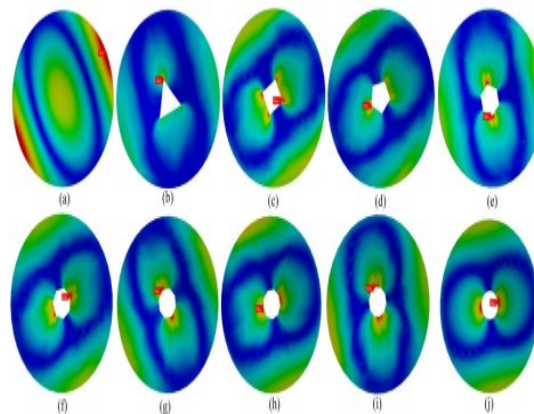
Table 5. Harmonic response analysis results of cross-ply circular plates.

Parameter	No Cut-Out	Equilateral Triangular Cut-Out	Square Cut-Out	Regular Pentagon Cut-Out	Regular Hexagon Cut-Out
Phase Shift (°)	89.464	95.296	93.633	93.725	90.644
Maximum Stress (MPa)	126.560	173.690	83.656	113.260	95.264
Maximum Displacement (mm)	2.5323	1.7661	1.4321	1.6046	1.4527
Parameter	Regular Heptagon Cut-Out	Regular Octagon Cut-Out	Regular Nonagon Cut-Out	Regular Decagon Cut-Out	Circular Cut-Out
Phase Shift (°)	89.39	90.338	92.387	93.834	88.946
Maximum Stress (MPa)	84.344	93.996	94.369	74.814	81.338
Maximum Displacement (mm)	1.3339	1.4988	1.5501	1.2476	1.3455

Table 6. Harmonic response analysis results of angle-ply circular plates.

Parameter	No Cut-Out	Equilateral Triangular Cut-Out	Square Cut-Out	Regular Pentagon Cut-Out	Regular Hexagon Cut-Out
Phase Shift (°)	89.511	89.64	93.73	90.008	89.789
Maximum Stress (MPa)	129.550	175.810	116.430	112.710	99.445
Maximum Displacement (mm)	2.5517	1.7805	1.4391	1.6079	1.4481
Parameter	Regular Heptagon Cut-Out	Regular Octagon Cut-Out	Regular Nonagon Cut-Out	Regular Decagon Cut-Out	Circular Cut-Out
Phase Shift (°)	90.35	88.481	91.606	89.759	92.84
Maximum Stress (MPa)	80.051	85.487	95.635	76.639	82.252
Maximum Displacement (mm)	1.3405	1.5032	1.5526	1.2545	1.3541

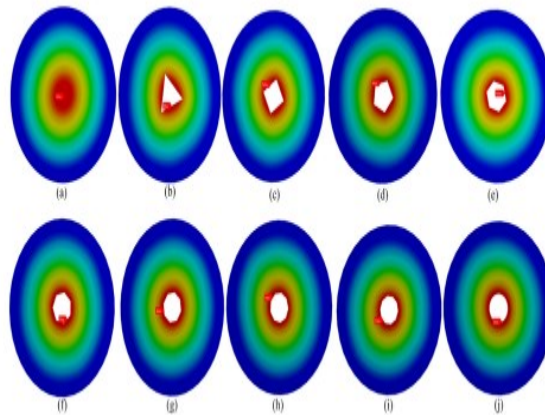
The phase shift has been marginally impacted by the fiber angles, as shown in Tables 5 and 6. The cross-ply circular structure with a triangular cut-out evaluated to have the maximum value (95.2960), while the angle-ply circular structure with a regular octagon cut-out obtained the minimum value (88.4810). The cross-ply structure with a regular decagon cut-out had the lowest stress value (74.814 MPa), whereas the angle-ply building with a central equilateral triangle cut-out had the greatest stress value (175.810 MPa). In the square cut-out structure, the stress value is 83.656 MPa for the cross-ply orientation and 116.43 MPa for the angle-ply sequence, which is the only substantial variance in stress values among Fiber orientations. Other structures have also been affected by the change in Fiber orientation. Although these changes are apparent, they are quite little (less than 5 MPa) as compared to the square hole. The displacement measurements show that the angle-ply structure without the cut-out moved the most, with a value of 2.5517 mm, while the cross-ply structure with the regular decagon cut-out moved the least, with a value of 1.2476 mm. The influence of fiber orientation on the structure's displacement is negligible, since the structure without cutouts had the largest displacement difference of 0.0194 mm. The cut-form outs significantly affect the structure's displacement sensitivity, as may be concluded. All configurations show that there is no strict correlation between the number of cut-out edges and the direction of the fiber when analyzed using phase shift values. A higher number of cut edges results in a higher degree of stress. But unlike phase changes, stress levels typically go down as the number of cut-out edges goes up for all stacking sequences. The displacement response, which reflects the stress trend, diminishes with increasing edge cut-out number in both Fiber orientations. A regular pattern in the distribution of stresses is shown by the results of the harmonic response analysis. Circular plates with cross-ply and angle-ply constructions



show their stress patterns in the figure. 4.

Circular cross-ply and angle-ply systems exhibit harmonic stress distributions (Figure 4). When any kind of central cut-out is present, as shown in Figure 4, the strongest stress moves from the structure's edges to the region immediately around the cut-out. When the cut-outs are quite diverse in shape, the stress may be felt in many distinct places. The blue region experiences the least amount of stress, at around 0 MPa, whereas the green, yellow, and red regions exhibit the highest levels of stress. Figure 4 demonstrates that the amount of light green and green regions becomes more uniform as the number of cut-out edges increases. As a result, the distribution is most uniform in the circular cut-out. On the other hand, circular structures with holes also have their stress distributions changed by the cut-out shape. According to Tables 5 and 6, the structures with an equilateral triangular cut-out have the highest stress values. However, when the stress becomes closer to zero in the blue zone, there is a rapid decrease. The cutout's corners or edge will always have the most stress, regardless of its shape. Although the displacement zones are same in cross-ply and angle-ply structures, the displacement

values differ. The displacement maps for circular plates with cross-ply and angle-ply constructions are



shown in Figure 5.

Figure 5. Plots of displacement for circular cross-ply and angle-ply constructions under harmonic stress.

Displacement reactions of all structures function similarly, as shown by the plots in Figure 5, independent of the presence or form of the cut-out. On top of that, the forms of the initial modes of all structures are identical to the displacement plots of all structures.

CONCLUSION

This research investigates the fundamental natural frequency and harmonic response of thin composite circular constructions with various cut-out configurations. The following may be inferred from the data:

Regardless of the fiber's orientation, the fundamental frequency values tend to increase as the cut-out form approaches a full circle. There is little influence of cut-out geometry on phase shift independent of fibre polarity. • Displacement responses are typically less as opening shapes approach a circle. The least displacement is shown in a typical decagon-cut building, whereas the most is seen in an equilateral triangle-cut construction.

In terms of the displacement response distribution, there was zero link with fibre orientation, cutout shape, or presence. The graphs representing the displacement response and the fundamental mode are in perfect accord with each other since the peak response occurred at the fundamental frequency. The displacement response of the fiber is somewhat insensitive to its orientation.

In general, the stress value trend is decreasing as the opening form approaches a circle. Under normal circumstances, the stress levels are lowest in an equilateral triangle cut-out and greatest in a conventional decagon cut-out. Even with the square cut-out construction, the influence of fibre orientation on maximum stress values is small.

Because of the shape of the cut-out, the stress distribution is significantly different. As the form of the aperture becomes closer to that of a full circle, the stress distribution becomes more consistent and constant. As the number of cut-out edges increases, the areas with stress values between zero and maximum become more noticeable.

Because of the opening, the structure's core, not its edges, takes the brunt of the load.

REFERENCES

[1] Jived et al. (2018) collaborated with Viswanathan and Nurul Izyan and Aziz and Lee. Free vibration of cross-ply laminated plates based on higher-order shear deformation theory. *Steel and Composite Structures*, volume 26, issue 4, pages 473–484.

In 2021, Gonenli and Das published a paper. Locating cracks in plate frame constructions affects their buckling and dynamic stability. Article number: 311 in the *Brazilian Society of Mechanical Sciences and Engineering Journal*, volume 43, issue 3.

the third Publication Year 2017 by Yui Y., Zhang S., Li H., Wang X., and Tiang Y. The ANSYS-based modal and harmonic response study of the ditch device's essential components. *Journal of Procedia Engineering*, 174: 956-964.

In 2019, Jiaqiang et al., together with Liu, Zhang, Zuo, Hu, and Wei, published a study. The study of the harmonic response to wind-induced vibration in a large-dish solar thermal power generating system. Paper published in *Solar Energy*, volume 181, pages 116–129.

In 2020, Kumar and Sarangi published a paper. How a finite element analysis of a functionally graded beam reinforced with carbon nanotubes responds harmonically. The citation is from *Materials Today: Proceedings*, volume 44, issue 6, pages 4531–4536.

Wen, B., Duan, T., Ma, H., Zeng, J., and Chen, K. 2019. Examination of the vibrational reaction to the run-up of a broken, spinning compressor blade. *Physical and Electrical Signal Processing* 118: 568-583.

The study of harmonic response of symmetric laminated composite beams with various boundary conditions was conducted by Kırıl in 2014. Published in the journal *Science and Engineering of Composite Materials*, volume 21, issue 4, pages 568-583.

[8] In 2019, Gawryluk, Mitura, and Teter published a study. A composite beam subjected to harmonic excitation using a multi-functional force actuator and spinning at a constant speed provides a dynamic response. *Journal of Composite Structures*, Volume 210, Pages 956–662.

[9] In 2020, Abed and Majeed published a study. The impact of boundary circumstances on the harmonic response of laminated plates. Published in *Composite Materials and Engineering*, volume 2, issue 2, pages 125–140.

In 2021, Çeçen and Aktaş conducted an investigation of the modal and harmonic responses of newly reinforced concrete railway sleepers made of CFRP laminate. *Science and Engineering Citation*: 127: 105471.

In 2020, Oke and Khulief published a study. Composite pipes with thinning within the walls investigated dynamically as they transport fluid. The referenced article is published in the *Journal of Engineering Mechanics* and has the DOI: 04020118.

Referenced in [12] Zhang et al. (2018). Analysis of linked plate structures' harmonic responses by use of the dynamic stiffness technique. Article 127: *Thin-Walled Structures*, pages 402-415.

In 2020, Yulin, Lizhong, and Zhou published a study. A three-beam system subjected to a shifting load/mass-spring and including intermediate elastic connections reacts dynamically. "Earthquake Engineering and Vibration" (1992, 2nd edition), pages 377–395.

Version 18.2 of ANSYS@ Workbench [14]. In 2010, Petyt published a paper. *Finite Element Analysis: An Overview*. Oxford: Oxford University Press, 2002. Zhang, P., Sun, X., Qiao, H., and Lin, K. 2021. Assessment of elastic plates with various cuts using high-order free vibration theory. Published in the *Archive of Applied Mechanics*, volume 91, pages 1837–1858, paper number.

Albassam, B. (2021) [15]. Vibration control of a linear flexible beam structure stimulated by numerous harmonics. 9(4B): 410-427. Journal of Engineering Research.

In 2018, Çelebi, Yarımabaç, and Baran published a study. Investigation of nonuniform cross-sectional inhomogeneous rods by means of forced vibration. Engineering Research Journal, Volume 6, Issue 3, Pages 189–202.

[17] An article published in 2020 by Sivandi-Pour, Farsangi, and Takewaki. Vibration Frequency Estimation for Structural Floors by the Integration of AI and Finite Element Analysis. Published in the Journal of Engineering Research, volume 8, issue 3, pages 1-16.